

Supplementary Material to

Molecular Dynamic Simulations of OH-Stretching Overtone Induced

Photodissociation of Fluorosulfonic and Chlorosulfonic Acid

Priyanka Gupta

*Department of Chemistry, University of Otago, P.O. Box 56,
Dunedin, New Zealand*

Joseph R. Lane

*Department of Chemistry, University of Waikato, Private Bag 3105,
Hamilton, New Zealand*

Henrik G. Kjaergaard*

*Department of Chemistry, University of Copenhagen, Universitetsparken 5,
DK-2100 Copenhagen Ø, Denmark*

Table S1: Calculated CC-VSCF frequencies (in cm^{-1}) for the OH-stretching SOH-bending and OH-stretching OSOH-torsion combination states in FSO_3H .

OH-stretching state	$\text{OH}_{\text{str}} + \text{SOH}_{\text{bend}}$	$\text{OH}_{\text{str}} + \text{OSOH}_{\text{tors}}$
v=5	18243	17385
v=6	22190	21331
v=7	26928	26069

Table S2: Selected geometric parameters (in Angstroms and degrees) for the dissociative transition state of FSO₃H and ClSO₃H.

Parameter	PM3	MP2/TZP	CCSD(T)/AV(T+d)Z
FSO₃H			
$R_{\text{O-H}}$	1.3198	1.1709	1.2379
$\theta_{\text{H-O-S}}$	91.38	91.96	84.11
$\phi_{\text{H-O-S-O}}$	100.21	99.91	99.61
$R_{\text{S-X}}$	1.7951	2.2437	1.9780
ClSO₃H			
$R_{\text{O-H}}$	1.3249	1.2142	1.2854
$\theta_{\text{H-O-S}}$	103.05	98.36	89.13
$\phi_{\text{H-O-S-O}}$	98.14	100.26	101.18
$R_{\text{S-X}}$	2.5164	2.8835	2.4146

Table S3: Harmonic frequencies (in cm^{-1}) for the dissociative transition state of FSO_3H and ClSO_3H .

Mode	PM3	MP2/TZP	CCSD(T)/AV(D+d)Z
FSO₃H			
1	1408	2044	1951
2	1051	1452	1393
3	942	1260	1228
4	806	999	958
5	793	991	944
6	651	701	686
7	553	630	607
8	402	467	483
9	359	449	458
10	343	326	331
11	219	215	219
12	2306i	1478i	1565i
ClSO₃H			
1	1688	2219	1603
2	1134	1373	1374
3	968	1124	1217
4	701	1010	946
5	696	958	749
6	507	692	569
7	394	536	500
8	373	445	445
9	350	391	441
10	137	307	221
11	127	256	167
12	1917i	1857i	1533i

Table S4: Selected geometric parameters (in Angstroms and degrees) for the hydrogen-hopping transition state of FSO₃H and ClSO₃H.

Parameter	PM3	MP2/TZP	CCSD(T)/AV(T+d)Z
FSO₃H			
$R_{\text{O-H}}$	1.3518	1.2942	1.2976
$\theta_{\text{H-O-S}}$	85.37	73.38	73.39
$\phi_{\text{H-O-S-O}}$	130.14	134.60	132.99
$R_{\text{S-X}}$	1.5405	1.6017	1.54847
ClSO₃H			
$R_{\text{O-H}}$	1.3689	1.2969	1.2933
$\theta_{\text{H-O-S}}$	85.99	73.64	73.70
$\phi_{\text{H-O-S-O}}$	129.26	129.51	129.38
$R_{\text{S-X}}$	2.0664	2.0567	2.0104

Table S5: Harmonic frequencies (in cm^{-1}) for the hydrogen-hopping transition state of FSO_3H and ClSO_3H .

Mode	PM3	MP2/TZP	CCSD(T)/AV(D+d)Z
FSO_3H			
1	1152	2231	2138
2	946	1410	1351
3	873	1164	1119
4	808	1039	1004
5	750	971	938
6	640	780	791
7	456	676	654
8	391	493	498
9	353	463	470
10	295	412	402
11	252	307	310
12	2443i	1874i	1928i
ClSO_3H			
1	1110	2219	2123
2	931	1373	1319
3	846	1124	1077
4	803	1010	970
5	720	958	931
6	518	692	669
7	450	536	531
8	366	445	452
9	344	391	387
10	248	307	300
11	225	256	258
12	2278i	1857i	1920i

Figure S1: PM3 snapshots of the dissociation of FSO₃H. The simulation is evaluated after excitation to the $\nu = 5$ OH+SOH combination state.

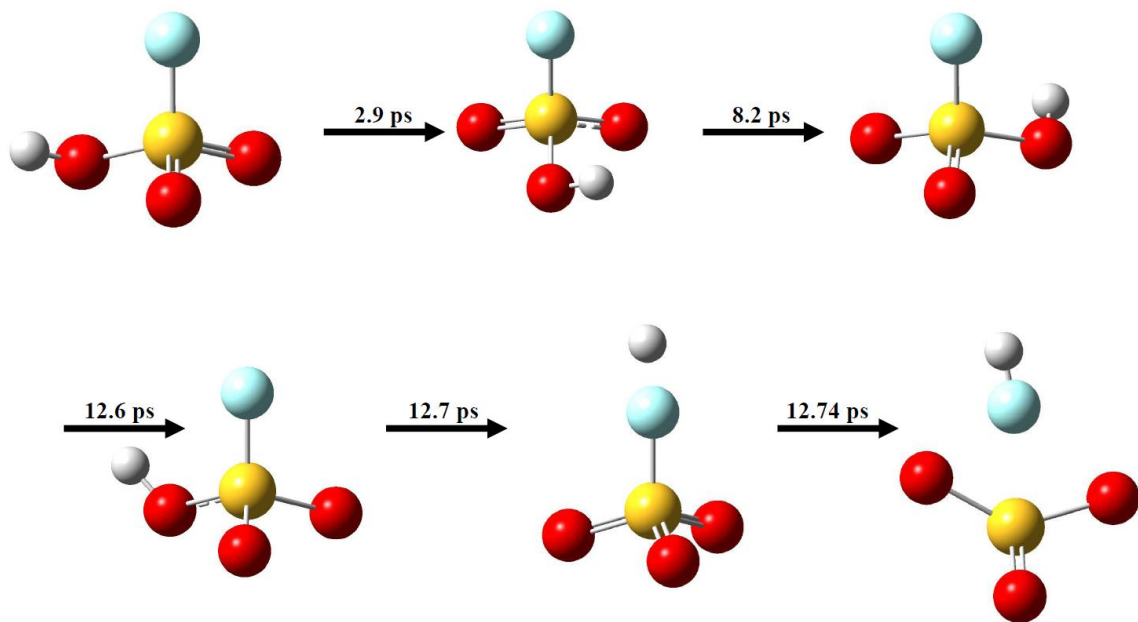


Figure S2: PM3 snapshots of the dissociation of FSO₃H. The simulation is evaluated after excitation to the $\nu = 5$ OH+OSOH combination state.

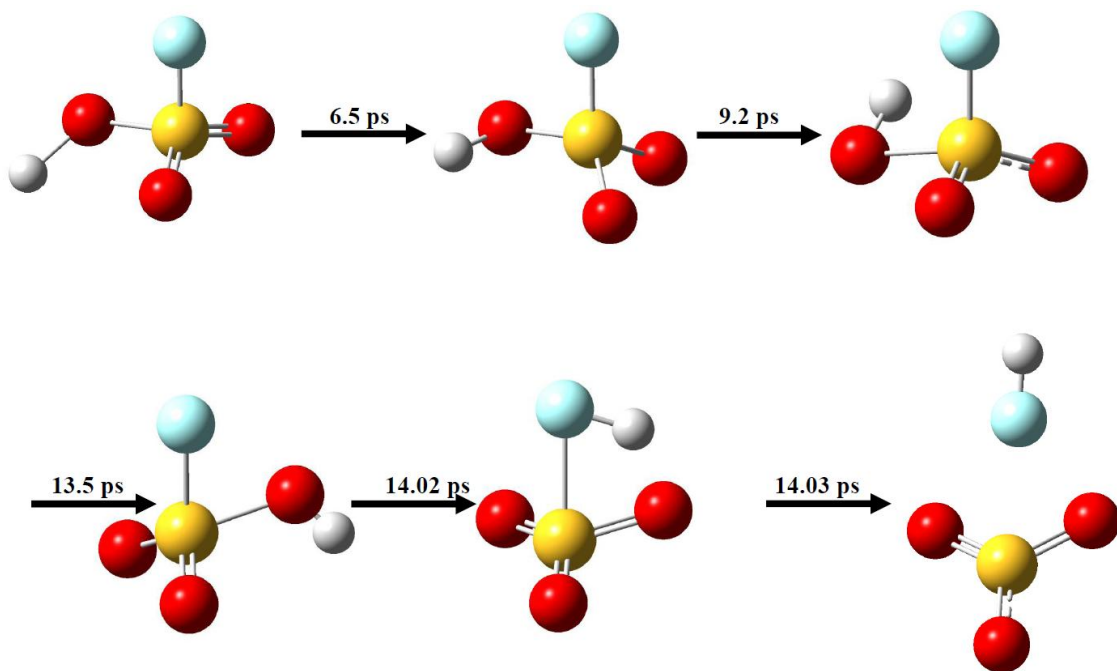


Figure S3: PM3 snapshots of hydrogen-hopping in FSO₃H. The simulation is evaluated after excitation to the $\nu = 5$ OH+SOH combination state.

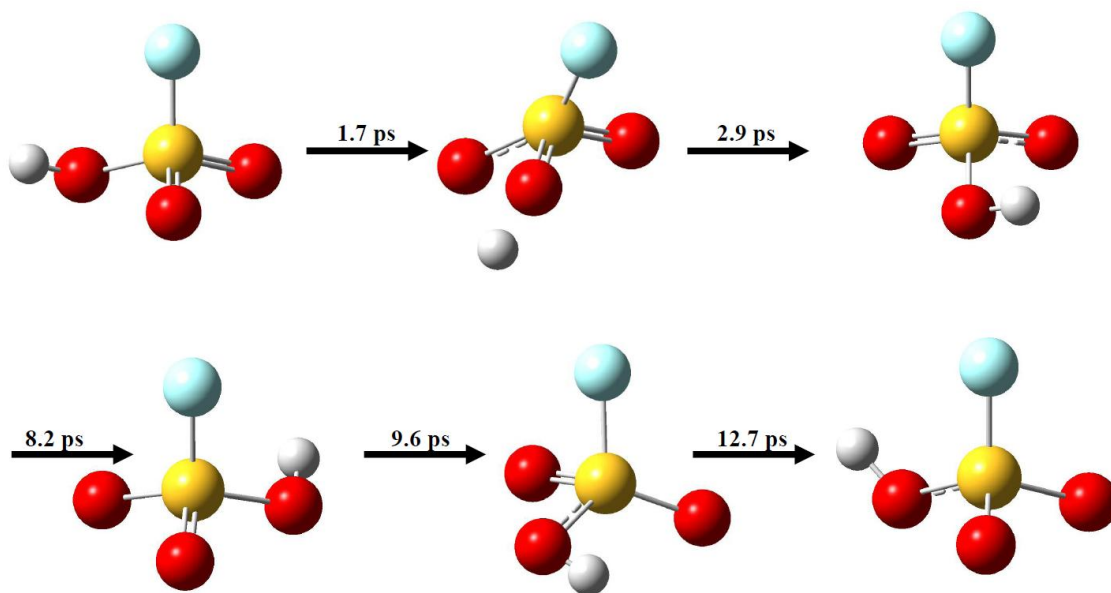


Figure S4: PM3 snapshots of hydrogen-hopping in FSO₃H. The simulation is evaluated after excitation to the $\nu = 5$ OH+OSOH combination state.

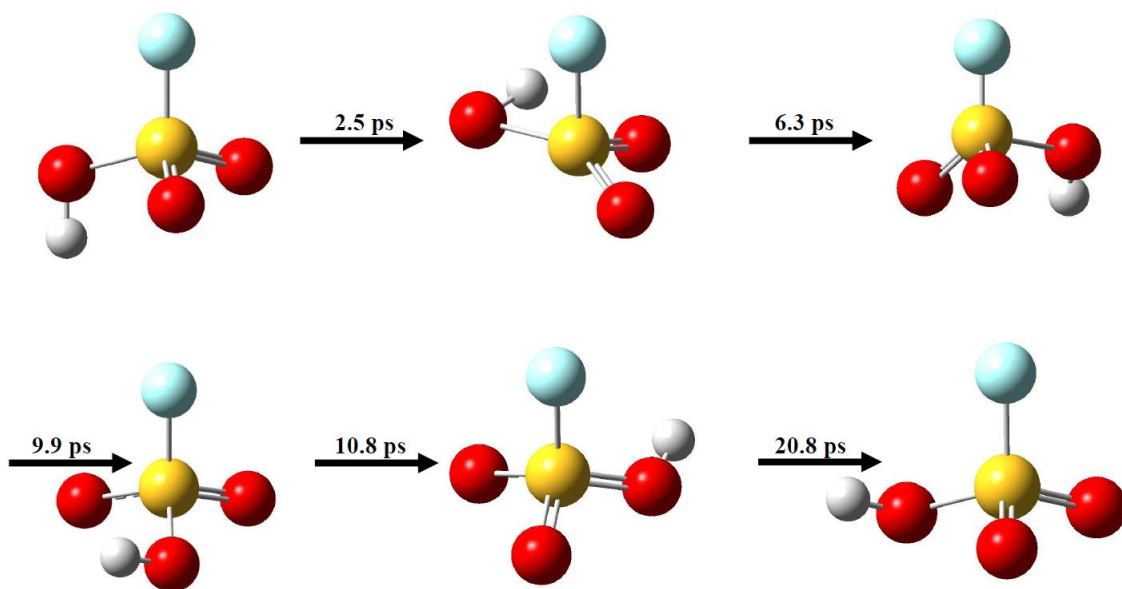


Figure S5: The time distribution of dissociation events for the PM3 $v = 5$ OH+SOH and OH+OSOH combination state trajectories of FSO₃H.

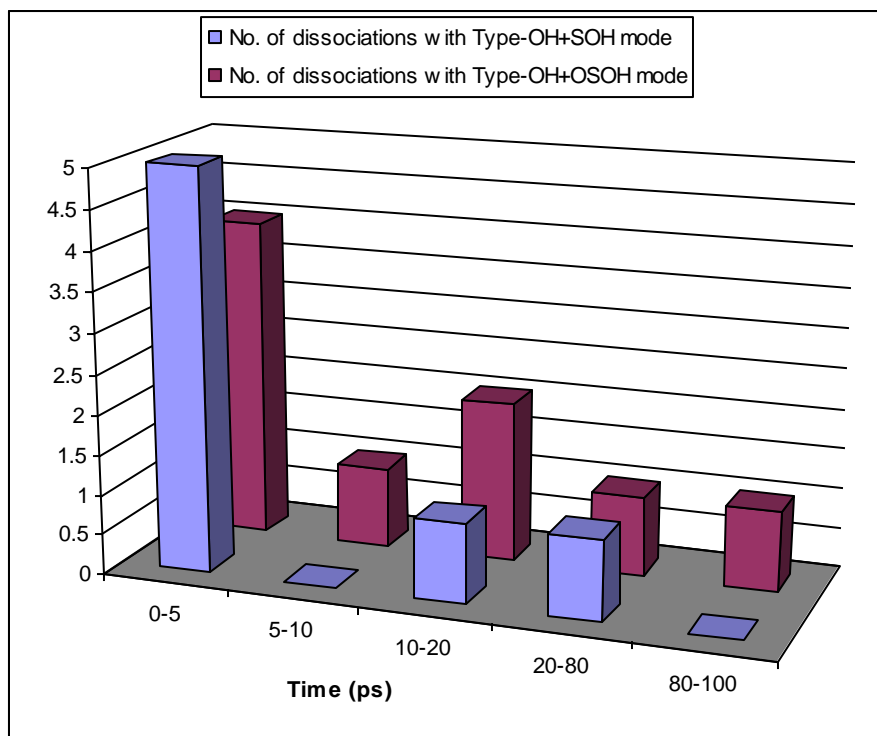


Figure S6: The time distribution of dissociation events for the PM3 $v = 6$ OH+SOH and OH+OSOH combination state trajectories of FSO₃H.

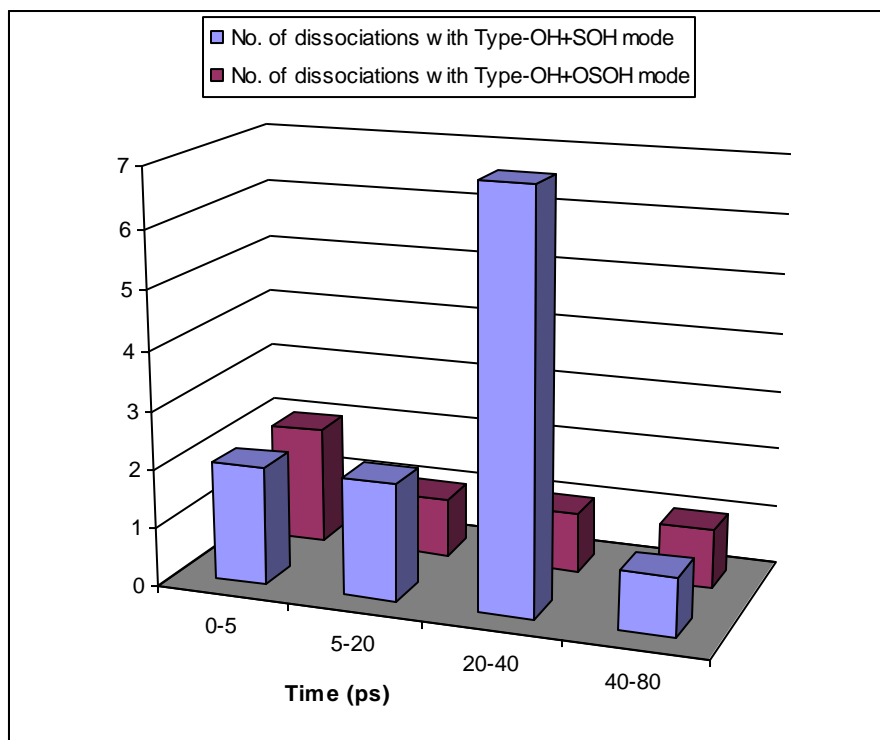


Figure S7: The time distribution of dissociation events for the PM3 $v = 7$ OH+SOH and OH+OSOH combination state trajectories of FSO₃H.

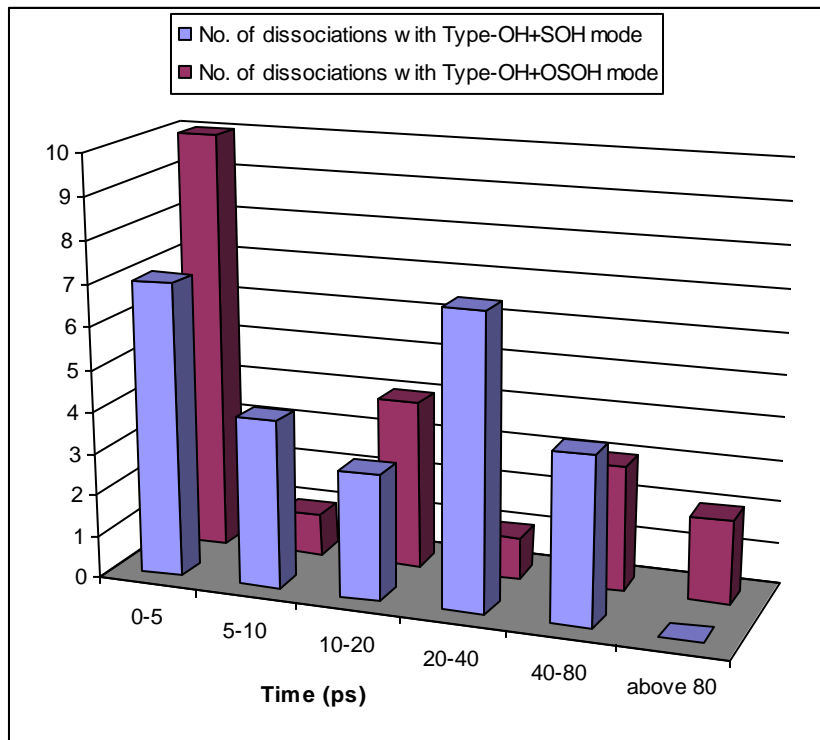


Figure S8: The time distribution of dissociation events for the MP2/TZP $\nu=5$, $\nu=6$ and $\nu=7$ OH-stretching trajectories of FSO_3H .

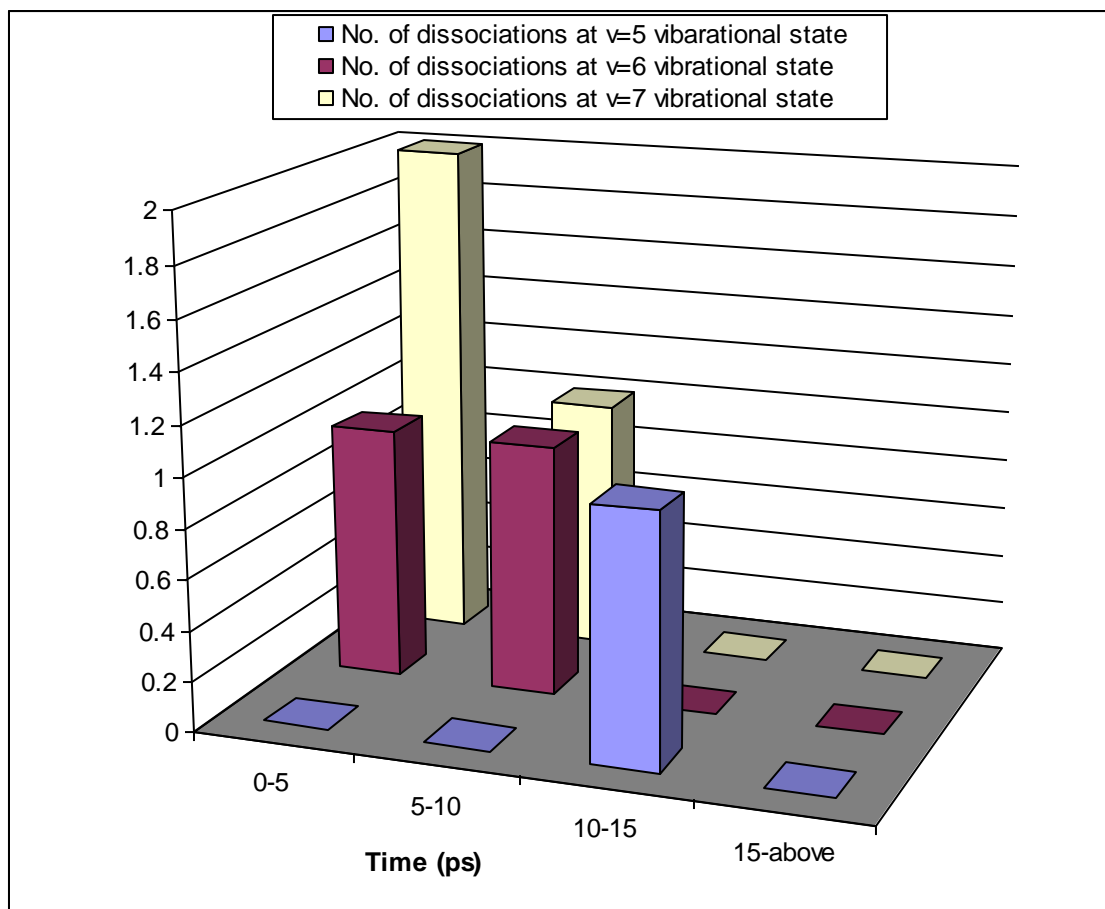


Figure S9: The time distribution of dissociation events for the PM3 $v=4$, $v=5$ and $v=6$ OH-stretching trajectories of ClSO_3H .

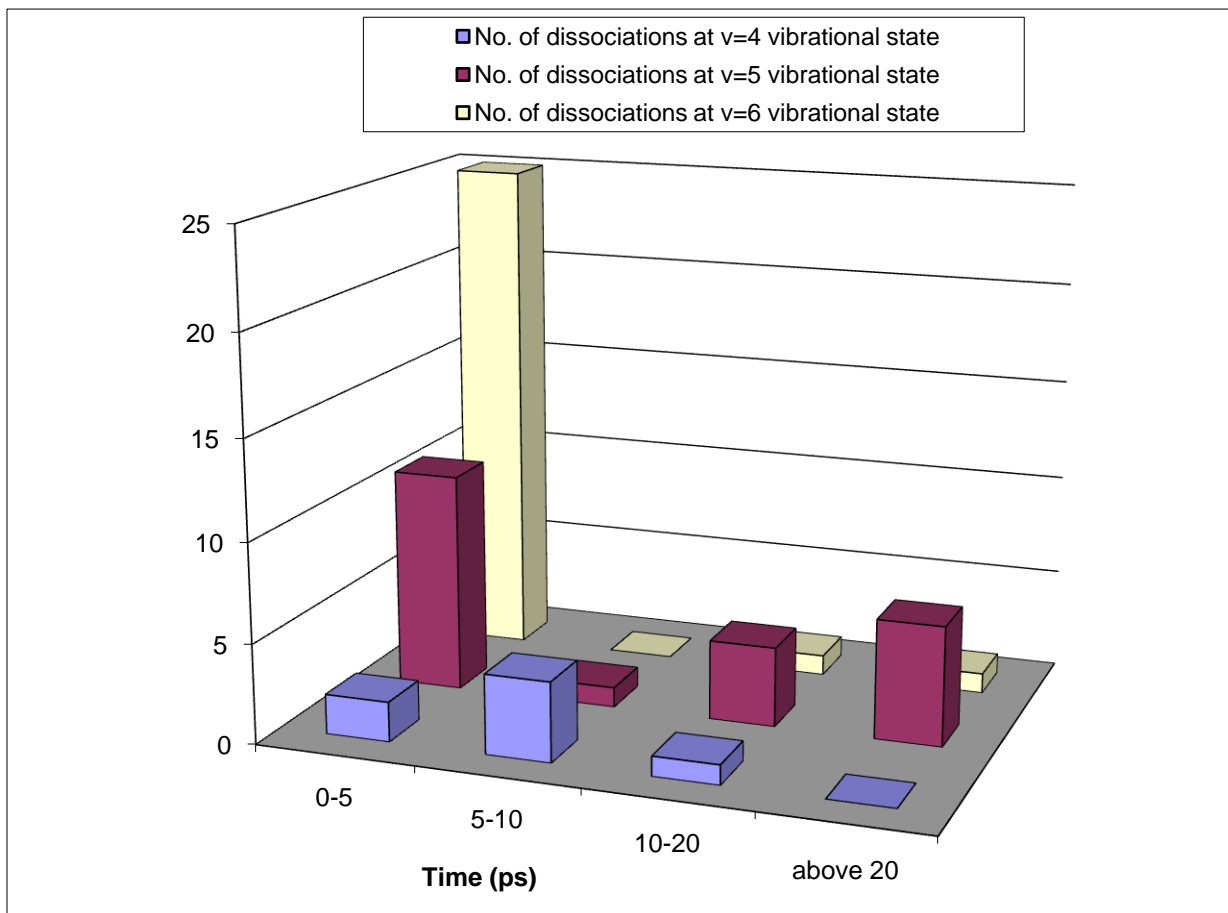


Figure S10: The time distribution of dissociation events for the MP2/TZP $\nu=4$, $\nu=5$ and $\nu=6$ OH-stretching trajectories of ClSO_3H .

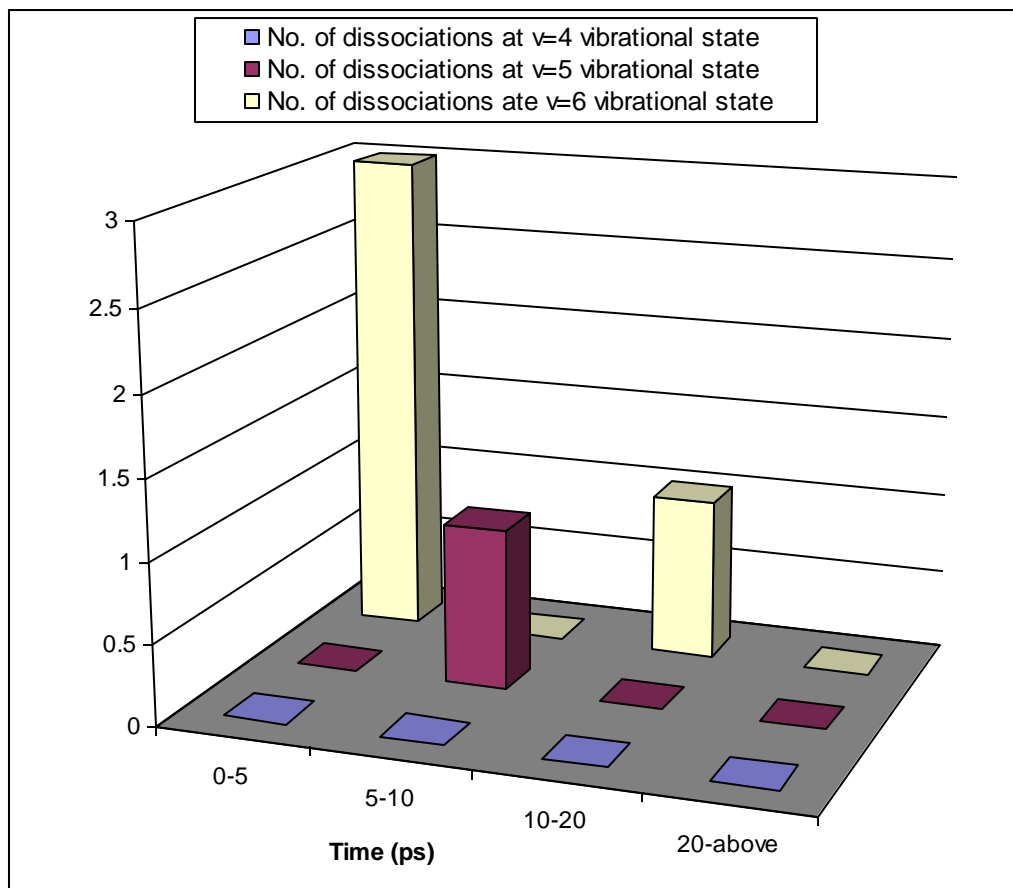


Figure S11: The time distribution of the first hydrogen-hopping event exhibited in PM3 trajectories for the $\nu = 5$, $\nu = 6$ and $\nu = 7$ OH-stretching states of FSO_3H .

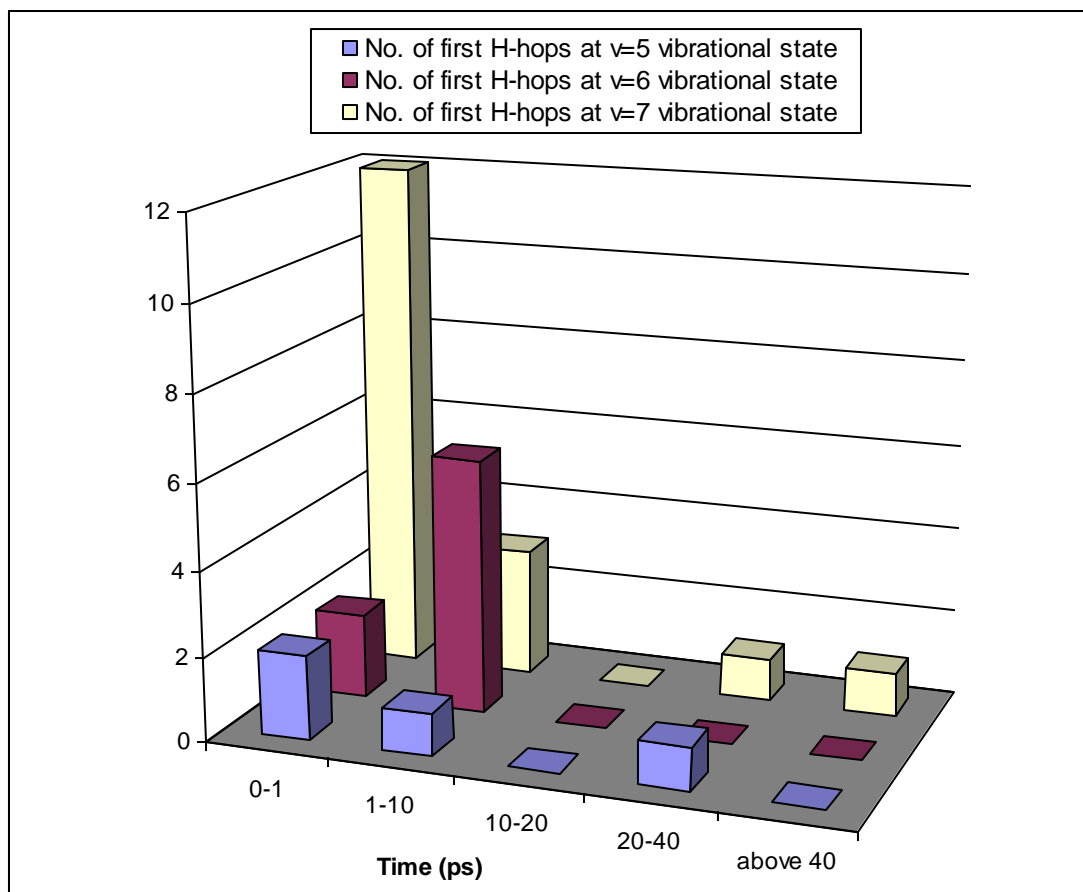


Figure S12: The time distribution of the first hydrogen-hopping event exhibited in PM3 trajectories for the $v = 5$ OH+SOH and OH+OSOH combination states of FSO₃H.

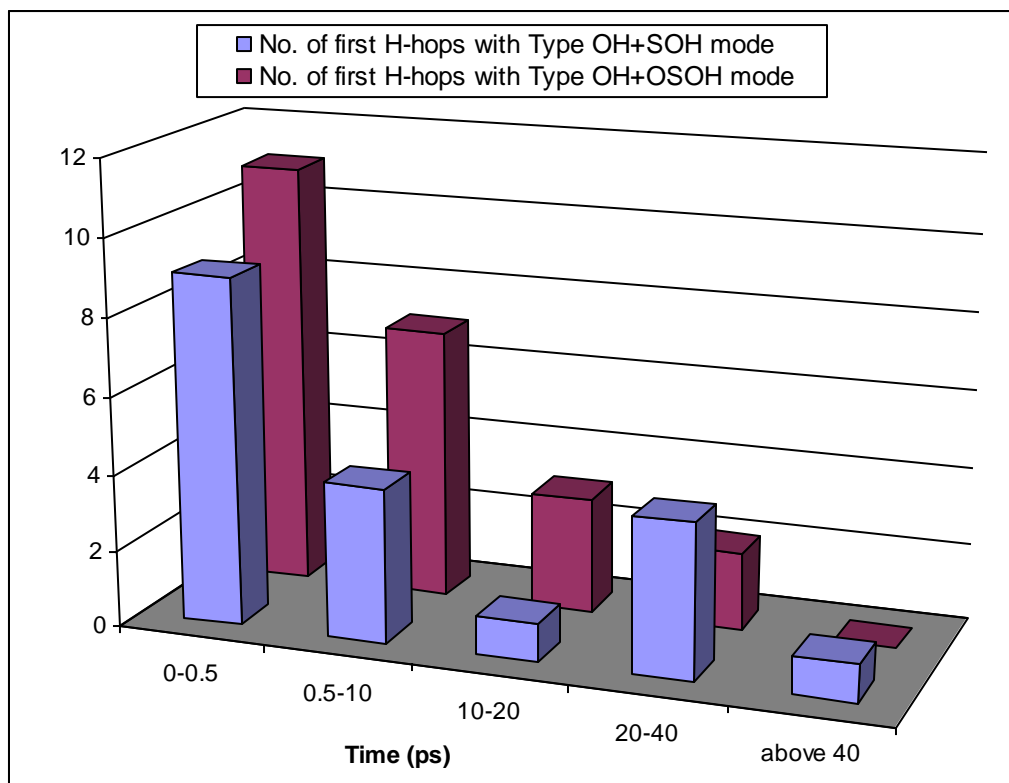


Figure S13: The time distribution of the first hydrogen-hopping event exhibited in PM3 trajectories for the $v = 6$ OH+SOH and OH+OSOH combination states of FSO₃H.

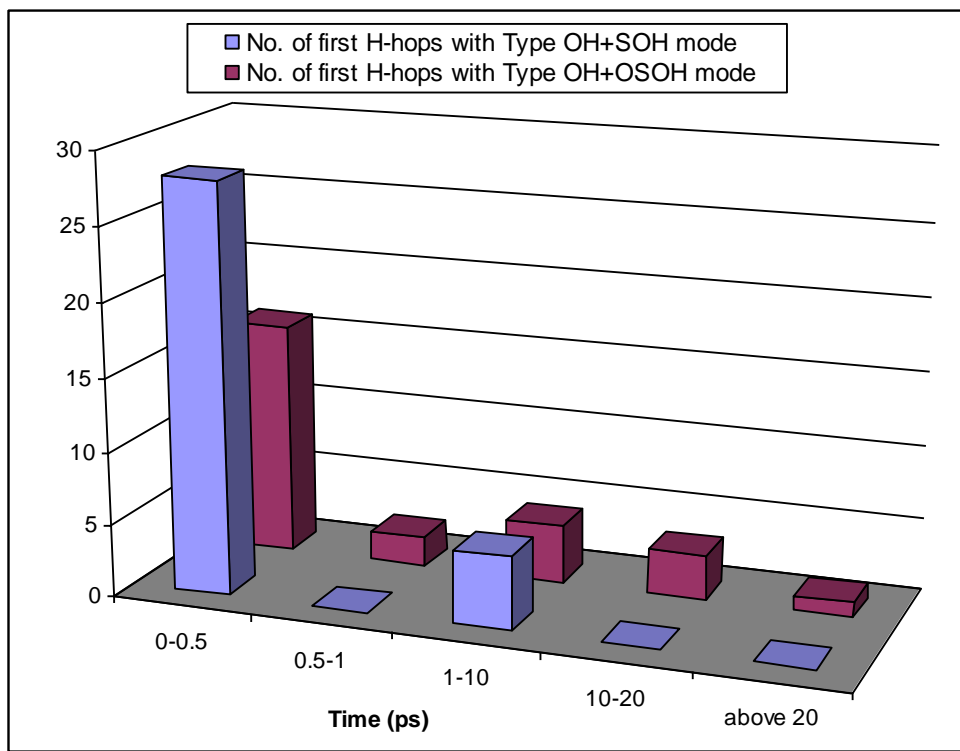


Figure S14: The time distribution of the first hydrogen-hopping event exhibited in PM3 trajectories for the $v = 7$ OH+SOH and OH+OSOH combination states of FSO₃H.

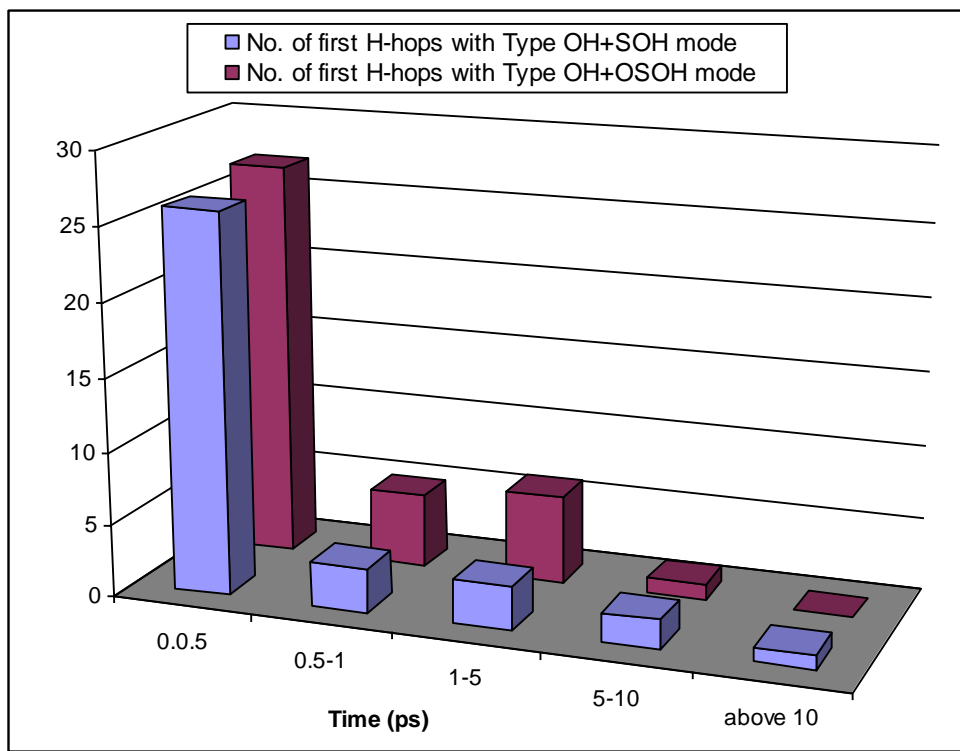


Figure S15: The time distribution of the first hydrogen-hopping event exhibited in MP2/TZP trajectories for the $\nu = 5$, $\nu = 6$ and $\nu = 7$ OH-stretching states of FSO₃H.

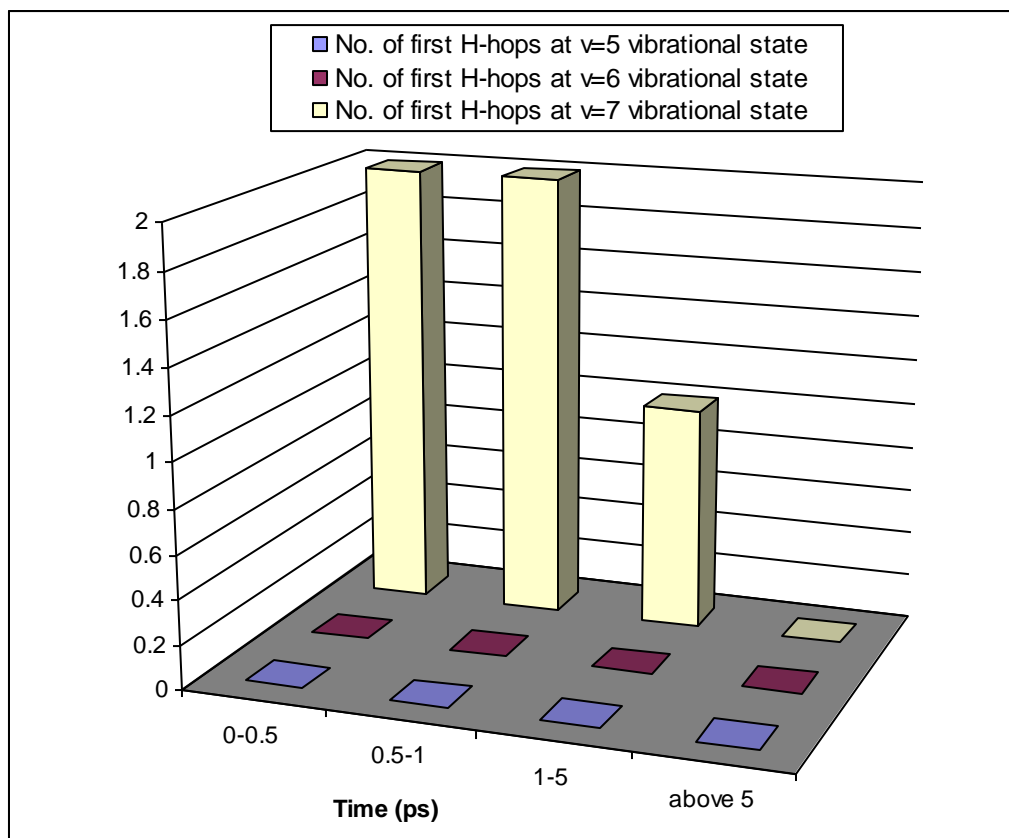


Figure S16: The time distribution of the first hydrogen-hopping event exhibited in PM3 trajectories for the $\nu = 4$, $\nu = 5$ and $\nu = 6$ OH-stretching states of ClSO_3H .

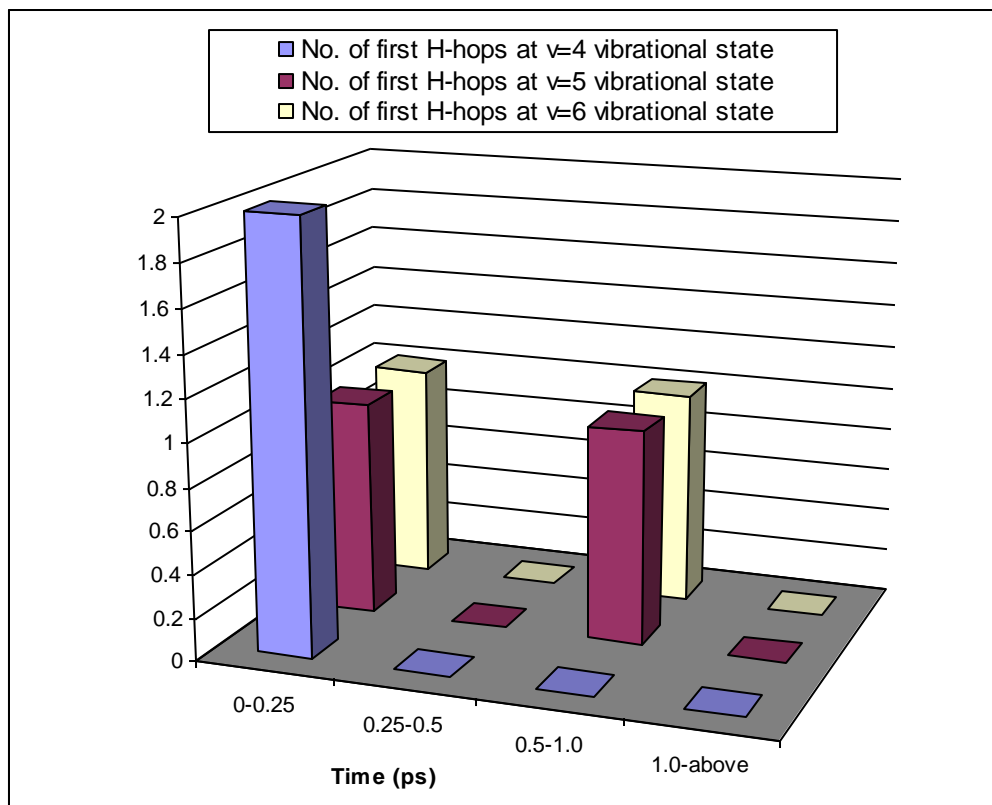


Figure S17: The time distribution of the first hydrogen-hopping event exhibited in MP2/TZP trajectories for the $\nu = 4$, $\nu = 5$ and $\nu = 6$ OH-stretching states of ClSO_3H .

